# Passive flow control in wind turbine blade by geometrical optimization of vortex generator

*Karthik* Jayanarasimhan[1*], *Navin Kumar* Balasubramanian[2]

[1]Research Scholar, Institute of Mechanical Engineering, Saveetha School of Engineering, Saveetha Institute of Medical and Technical Sciences, Chennai 602105.
[2]Associate professor, Institute of Mechanical Engineering, Saveetha School of Engineering, Saveetha Institute of Medical and Technical Sciences, Chennai 602105.

**Abstract.** A wind turbine is a device that converts mechanical energy into electrical energy by its rotary action. In this paper, a wind turbine's lift and power characteristics are improved by employing a vortex generator as a passive flow control device on the surface of the wind turbine. A triangular vortex generator is used for this study for its simplicity in design and effective results. NACA 4418 airfoil is selected for the conceptual design by BEM (Blade Element Momentum theory), and geometrical modeling is carried out using SOLIDWORKS. Computational analysis of the blade with vortex generators is done using ANSYS CFX, and analysis on a clean blade is verified using Q Blade. The geometrical parameters considered for optimization are chordwise position ($x_{vg}$), Height ($h_{vg}$), and Inclination from the baseline($\beta_{vg}$), keeping fixed spacing ($s_{vg}$). By optimizing the design parameters, the lift and power increment is observed alongside a delay in the flow separation point, which agrees with the experimental results. This investigation can be extended to future unconventional shapes such as ogive, vane, and wishbone generators through wind tunnel and field tests.

## 1 Introduction

Energy conservation is the mandatory area to be focussed on in forthcoming years. Harvesting energy without carbon emissions is the greatest challenge many developed countries face. Energy consumption has skyrocketed to 95% in the timeline of 1980-2015 and is expected to be 250% consumption by the end of 2030. India uses more than 10% of its resources for wind energy[Fig 1a], on par with the global market. Coal [Fig 1b]is a significant energy module that depletes the atmosphere significantly. A wind turbine is one of the efficient ways to harvest green energy by lift generation in the blade leading to rotary motion. Besides having a significantly low carbon footprint, it houses the potential to support more jobs ranging from farmers to turbine blade designers in the coming decades.

Wind energy is one more reason for depriving our dependency on fossil fuels for energy generation. A wind turbine is one of the efficient means of harnessing green wind energy

*Corresponding author: karthikj9071.sse@saveetha.com

with a minimum negative impact on society. Wind turbine design has evolved through various phases such as Horizontal, Vertical, bladeless, and offshore turbines in past decades. Though many researchers study the aerodynamics of wind turbines [1], it still needs to be explored as the majority have tapped only the energy production by optimizing material, geographical placement, and structural analysis of wind turbine blades.

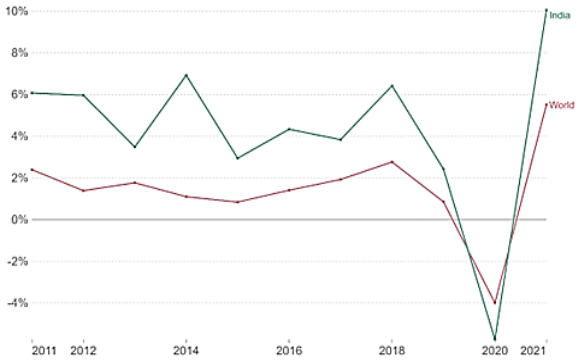


**Fig. 1(a).** Comparison of Wind energy consumption in the World vs. India in the past decade (2011-2021).

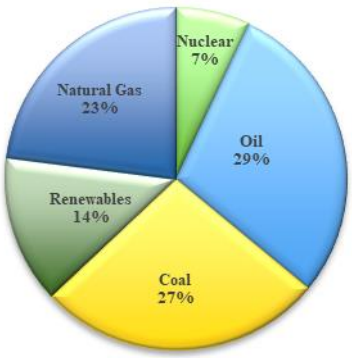


**Fig. 1(b).** Energy consumption trend in India in 2022-23.

Flow control is an exciting phenomenon in fluid dynamics research, catering to the opportunity to manipulate the flow under favorable conditions. They are categorized as active and passive flow control[2]. In active flow control, an actuation mechanism[3] influences the incoming flow, whereas passive flow control devices depend on their geometrical shape and position on the flow surface. There is no actuation mechanism and flow control is organically induced through geometrical characteristics.

A vortex generator is one of the essential passive flow control devices which primarily influences the incoming flow by geometry and position on the installed surface[4]. Research on vortex generators has roots in the late 1940s [5] using vane-type generators [6] for flow control in diffusers and airfoils. It paved the way for understanding the aerodynamic importance and influence of parameters such as vane angle[7] and separation distance[8] on the flow control of airfoils. Subsequent research on high-speed flows on various airfoils and aircraft is summarized by Lin[9]. Research on vortex generators have crossed leaps and

bounds in past decades, and with the advent of novel technologies[10] for computational analysis software such as ANSYS, OpenFOAM, and turbulence modeling such as RANS(Reynolds Average Navier Stokes Equation), LES(Large Eddy Simulation) and flow visualization methods such as PIV (Particle Image Velocimetry).

## 2 Methodology

The methodology involves a top-down approach starting from a literature survey on wind turbine blade design, the influence of vortex generators on various streamlined and bluff bodies, and effective optimization of geometrical parameters. The design of the wind turbine blades is preceded by airfoil selection and computational modeling. For the analysis, the NACA 4418[11] airfoil is chosen due to its maximum coefficient of lift $(C_L)_{max}$ of 1.727 and angle of attack ($\alpha$) of 6.5°.

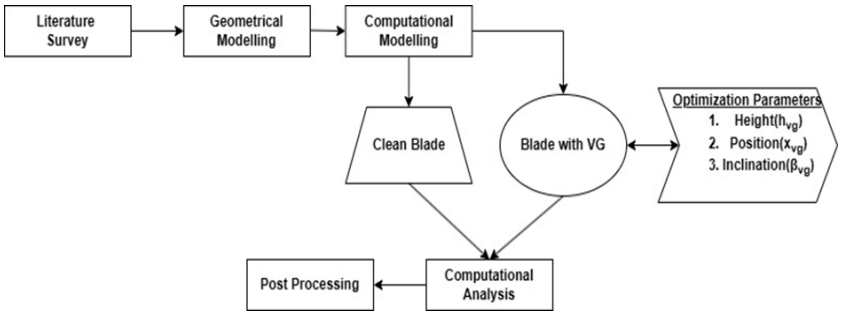


**Fig. 2.** Methodology.

## 3 Analysis of blade

### 3.1 2D Analysis of Airfoil

A preliminary study on 2D analysis of airfoil is executed to understand the flow over the airfoil, the influence of the position of separation points under varied conditions, and the dynamics behind the flow control mechanism. Computational domain Fig3(a) is designed in such a way that the far-field length is 60 times the chord length of the airfoil and the leading edge and trailing edge length are 30 times the chord length of the airfoil to visualize the flow over the airfoil conveniently. The meshing of the airfoil surface is a tedious process as the surface is unconventional, and impossible to generate a structured mesh. The structured mesh is tried for this airfoil surface by cloning the leading-edge surface to a certain height in the far-field boundary. Since airfoil flow is an external flow and the leading edge is a critical zone in analysis, a step mesh Fig3(b) is created near the airfoil's leading edge as the number of elements close to the leading edge will be higher to catch the flow properties accurately. The analysis shows that the flow separation zone approximates 70-90% of position to chord length (x/c).

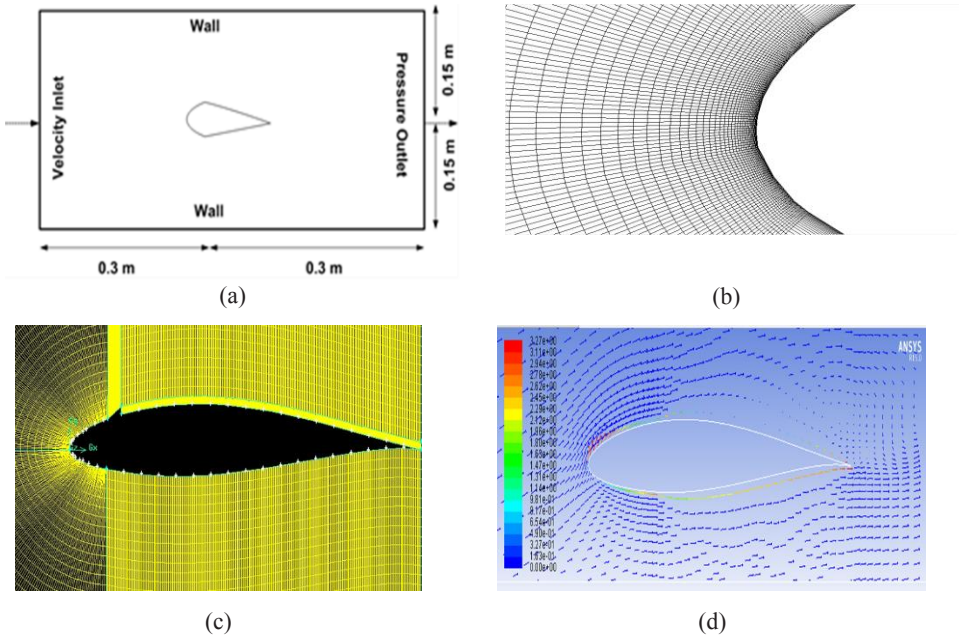


**Fig. 3.** (a) Computational Domain for airfoil (b) Step meshing of the airfoil (Zoom view) (c) Mesh of airfoil with Vortex generator (d) Flow separation point identified from velocity vectors.

### 3.2 Blade design by Blade Element Momentum Theory [BEM]

Geometrical modeling of the blade is done using SOLIDWORKS software, and computational analysis is executed using the ANSYS-CFX module. Blade Element Momentum Theory [BEM] calculates the design data for blade design. In this process, the blade surface is divided into considerably equal sections [Fig4], and an airfoil's sectional chord length and twist angle are calculated individually. From the individual section data, the blade design is modeled [Fig5] using SOLIDWORKS software

The Design Conditions are

1. Rotor Diamter = 0.48m
2. Length of Blade =0.225m
3. Rated Wind speed =12m/s
4. Design Lift coefficient = 1.03

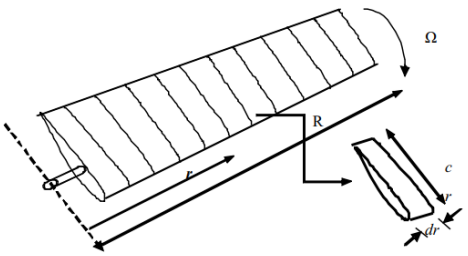


**Fig. 4.** Sectional view of blade [11] using Blade Element Momentum Theory with design conditions.

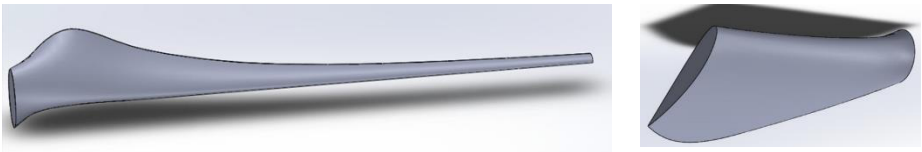

**Fig. 5.** Geometrical Modelling of Blade in Plain View and Cut View at z/h=0.25 [airfoil view].

### 3.3 Computational Domain

The isometric computational domain for the blade is generated and meshed in ANSYS CFX software. Periodic boundary conditions [12]are applied to the blade as it involves rotary motion and gives computational ease of analyzing the blade in the 120$^{o}$ quadrant domain. The velocity inlet boundary condition is applied in the front face of the domain, and the pressure outlet boundary condition is applied behind. Wall boundary conditions are applied on the covering surface with periodicity. CFD RANS(Reynolds Average Navier Stokes) model with k-ω SST[13] (Shear Stress Transport) turbulence is applied for the blade. Since the flow is external, this turbulence model gives appealing results with computational accuracy. The residual is fixed to be $e^{-6}$ for garnering accurate results.

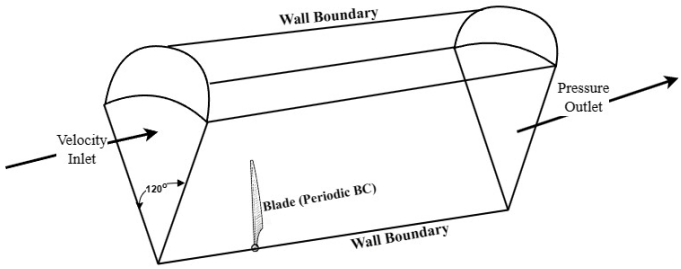


**Fig. 6.** Computational Domain of Blade.

### 3.4 Grid dependency

Grid study is one of the necessary processes in Computational analysis. It clarifies the number of elements to be incorporated in the structure to have meshed for noticeable results. Computational time can be saved mainly by performing grid dependency checks before the onset of any computational analysis. In this study, three different gids are designed, and results are studied. The 1$^{st}$ type of grid is the default reference mesh [Fig 7a]with 2 million triangular elements throughout the blade surface, and it yields a lift coefficient of 1.18(~1.9% error) in computational analysis with computational runtime of 2.3 hours. The 2$^{nd}$ type of grid is a course mesh with 1.2 million triangular elements yielding a lift coefficient of 1.078(~10.39% error) with computational runtime of 1.6 hours. The final grid type is a fine mesh with 3.3 million elements giving a lift coefficient of 1.20 with negligible error, but the computational time is 3.23 hours. The grid dependency study should be a balance between computational time and error percentile from the original value. Comparing the types of grids mentioned above, the reference grid with 2 million elements is selected for the analysis as it gives optimum results with minimum error and cumulatively less computational time.

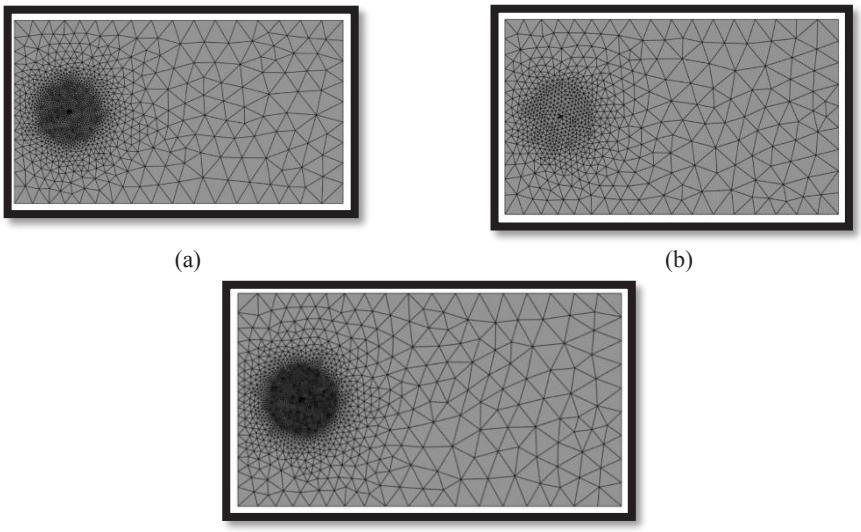


**Fig. 7.** Grid dependency study with **(a)** Reference mesh with $2x10^6$ elements, **(b)** Course mesh with $1.2x10^6$ elements, **(c)** Fine mesh with $3.34x10^6$ elements.

### 3.5 Design of Vortex Generator

A vortex generator is one of the essential passive flow control devices finding application in subsonic inlets of gas turbine engines, sedan cars[14], flat plate flows [15], and internal pipe flow such as S-duct due to its impeccable flow control performance and ease in design. A triangular vortex generator[16], [17] is selected for this study based on minimum complexity in design and maximum performance in external flows. A vortex generator design [18]involves various factors such as type, spacing, angle[7], position, length, and Height [19] of the generator. This study uses a counter-rotational triangular vortex generator[Fig 8] to optimize parameters Height, chordwise position, and inclination angle [20].

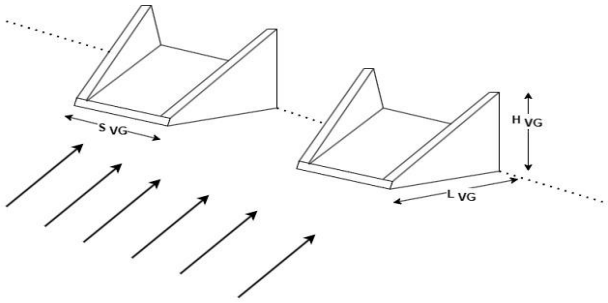


**Fig. 8.** Triangular Vortex Generator layout.

## 4 Results and Discussion

Computational analysis is conducted in NACA 4418 clean blade[11] (without vortex generators) at a rated wind speed of 12m/s.CFD results on lift coefficient($C_L$=1.20) agree with the theoretical value of lift coefficient ($C_{L\ theoretical}$ =1.209) with negligible error (~0.75%), forming the baseline benchmark for the optimized results. The optimization parameters taken for investigation are Chordwise position (70% 80% of x/c) of, Height to boundary layer thickness ratio ($H_{VG}$=δ,0.5δ), Inclination of vortex generator with the base surface($\beta_{VG}$ =15$^o$,18$^o$). The spacing between generators and pairs of generators is considered constant throughout the analysis. Triangular vortex generator is used in this investigation due to their simple design and accuracy in results.

An optimization table [Table 1] is created with possibilities of the variables mentioned above, and computational analysis is carried out with selected grid from grid dependence study and pre-processing variables for clean blade and blade with vortex generators

**Table 1.** Optimization table

| Case | Position (x/c) | Height ($H_{VG}$) | Inclination ($\beta_{VG}$) | Differential flow separation Point ($\Delta x_f$, $\Delta y_f$) | Lift Coefficient ($C_L$) |
|---|---|---|---|---|---|
| | % | mm | mm | mm | No unit |
| I | 70 | 0.5δ | 15 | -2. | 1.01 |
| II | 70 | δ | 15 | +4.78 | 0.99 |
| III | 70 | 0.5δ | 18 | -2 | 1.11 |
| IV | 80 | δ | 18 | -5.78 | 1.33 |
| Clean blade | - | - | - | - | 1.20* |

**Note**: In differential flow separation point, "+" indicates flow has separated beyond the conventional flow separation point, and "-" indicates flow has separated before the conventional separation point.

Computational analysis of a clean blade (without vortex generator) yields a lift coefficient 1.20(~0.25% error) at a rated speed of 12m/s.The flow over the clean blade [Fig 9a] experiences no reverse flow throughout the longitudinal contour surfaces. The vortex generator position in Case I [x/c=0.7;$h_{vg}$=0.5δ;$\beta_{vg}$=15 $^o$] has its flow separation point behind the conventional position by 2mm yielding a lower lift coefficient of 1.01(~16.1% less than conventional $C_L$*). The momentum transfer to the boundary hasn't sustained enough in Case II[x/c=0.7;$h_{vg}$=δ;$\beta_{vg}$=15$^o$] as the flow separates beyond the flow separation point by 4.78mm with the lowest lift coefficient among the optimizing cases. Case III [x/c=0.8;$h_{vg}$=0.5δ;$\beta_{vg}$=18 $^o$] gives the best results compared to other cases with differential separation of approximately 5mm behind the conventional separation point. This invariantly increases the lift coefficient of the blade to 1.33 (~10.833% increment compared to conventional $C_L$*). The optimized position of the vortex generator is, therefore, at 80% of chordwise length with 50% of boundary layer thickness at an inclination of 18$^o$ with baseline surface. The flow separation contour for the optimized position is depicted in Fig 9b, which explains the flow separation behind the baseline point.

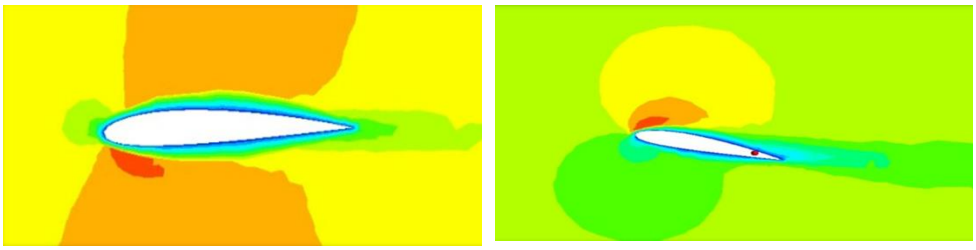

**Fig. 9.** Velocity variation of **(a)** Clean blade **(b)** Blade with vortex generator placed at optimized position [x/c=0.8;$h_{vg}$=0.5δ;$\beta_{vg}$=18 º].

Chordwise velocity variation is studied to understand the variation in the effect of flow separation in the blade's longitudinal axis for all the five cases mentioned above. The blade is cut at specified locations from z/c=0.4,0.5,0.6,0.8 and 0.9 for vortex generator cases I-IV to zero-in the impact location due to flow control in the vortex generator. The velocity variation in the cut view at z/c=0.4 and z/c=0.5 shows no effect on the vortex generator as their contours show no deviation in their path for all cases (Fig 10 a,b). The severity of flow separation onsets on z/c=0.6 with minimal deviation viewed in Case I [x/c=0.7;$h_{vg}$=0.5δ;$\beta_{vg}$=15 º] and Case II[x/c=0.7;$h_{vg}$=δ;$\beta_{vg}$=15 º] due to proximity of the vortex generator to the separation zone. At z/c=0.8, the highest velocity($V_{max}$=25.6m/s) is obtained in optimized Case-III, leaving a considerable impact on the remaining cases. Though z/c=0.9 shows appreciable variation in all the cases, the velocity falls short to a maximum of 24.9m/s due to poor vortex strength in affinity to the blade's surface.

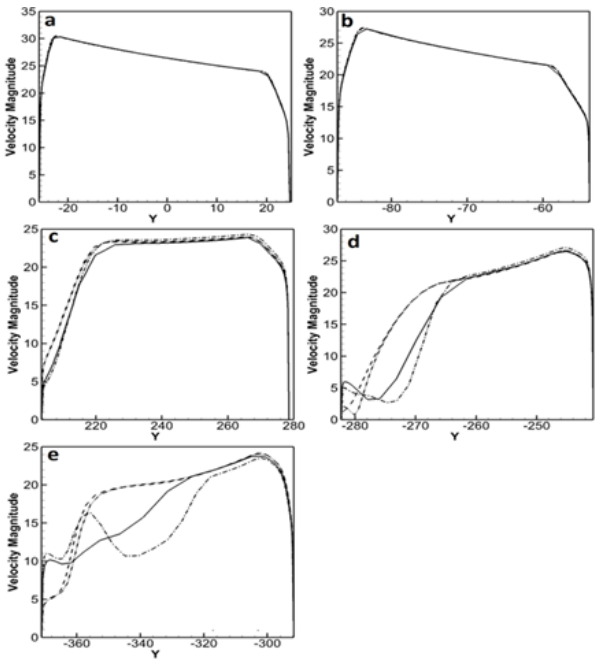


**Fig. 10.** Chordwise velocity variation of the blade in cut view for optimized cases at (a) z/c=0.4 (b) z/c=0.5 (c) z/c=0.6 (d) z/c=0.8 (e) z/c=0.9.

## 5 Conclusion

In this investigation, the effects of the geometrical parameters of the vortex generator on the power output of the wind turbine blade are summarised, and the optimized position of the vortex generator is suggested based on the results. The blade configuration is obtained using Blade Element Momentum Theory, and the angle of attack in each blade section is constant with maximum L/D. For the preliminary 2D airfoil analysis, the pre-processing is done using GAMBIT, and the post-processing is done in FLUENT. In 3D Computational analysis, an isometric domain is created with periodic boundary conditions and analyzed for various operating conditions. Computational results show blade with the optimized position of the vortex generator [Chordwise position x/c=0.8; Height of generator $h_{vg}$=0.5δ; Inclination of vortex generator with surface $\beta_{vg}$=18º] has a maximum lift coefficient ($C_L$=1.33), which is 29.12 % greater than actual lift coefficient of NACA 4418 clean blade ($C_L$=1.03). The maximum impact of the vortex generator is felt in the region of z/c=0.6-0.9, whereas the effective flow control is visualized at z/c=0.8 for all the optimized cases of the vortex generator. The investigation can be extended to field tests with different shapes of vortex generators, such as a wishbone and ogival, and monitor the effect in power coefficient and blade lift.

## References

1. K. Jayanarasimhan and V. Subramani-Mahalakshmi, *IntechOpen,***11** (2022).
2. A. S. Shehata, Q. Xiao, M. M. Selim, A. H. Elbatran, and D. Alexander, *Renew Energy.*,**113**, 369–392(2017).
3. Hoon Hwangbo , Yu Ding , Oliver Eisele , Guido Weinzierl , Ulrich Lang , Georgios Pechlivanoglou , *Renewable Energy,* **113**,1589-1597(2012).
4. G. W. Gyatt and A. Ron, *NASA Technical Report, DOE/NASA/0367-1* ,(1986).
5. H. Bruynes, *Patent: US2558816A*(1951).
6. I. Errasti, U. Fernández-Gamiz, P. Martinez-Filgueira, and J. M. Blanco, *J. Phys.: Conf. Ser*,**1222**(2019)
7. I. Ibarra-Udaeta, I. Errasti, U. Fernandez-Gamiz, E. Zulueta, and J. Sancho, *Appl. Sci*,**9** (2019).
8. J. Huang, S.Fu, Z.Xiao, and M. Zhang, *J. Fluid Sci. Technol*, **6**, 85–97(2011).
9. J. C. Lin, *Prog. Aerosp. Sci*, **38**, 389-420(2002).
10. P. Martínez-Filgueira, U. Fernandez-Gamiz, E. Zulueta , I. Errasti , B. Fernandez-Gauna, *Int. J. Hydrog. Energy*,**42**,17700-17712(2017)
11. M. Keerthana, M.Sriramkrishnan, T.Velayudham, A.Abraham, S.Selvirajan, K.M.Parammasivam, *J. Wind Eng*, **9**, 14-28(2012)
12. V. Dharani, N. Lavanya, and R. E. Ravalika, *Int. J. Mech. Eng. Technol*, **9**, 254–262(2018)
13. M. O. L. Hansen, C. M. Velte , S. Oye , R. Hansen , N. N. Sorensen , J. Madsen and R. Mikkelsen., *Wind Energy*, **19**, 563–567(2016).
14. M. Rasedul Islam, M. Amzad Hossain, M. Mashud, and M. Tanvir Ibny Gias, *Int J Sci Eng Res.,***4**,1298-1302(2013).

15. Z. Zhao, M. Chen, H. Liu, T. Wang, and B. Xu, *J. Renew. Sustain. Energy*, **3**, 033301 (2021).
16. U. Fernandez-Gamiz, J. Ruiz de Loizaga, I. Errasti, A. Boyano, E. Zulueta, and J. M. Lopez-Guede, *MATEC Web of Conf*, **307**, 01054(2020).
17. V. Yashodhar, G.Humrutha, M.Kaushik, and S.A.Khan, *IOP Conf. Ser: Materials Science and Engineering,***184**, 012007(2017).
18. O. M. Fouatih, M. Medale, O. Imine, and B. Imine, *EUR J MECH B/Fluids*, **56**,82–96(2016)
19. Devadasan N. P ,L.P.Rekha, *JETIR*, **5**,331-338(2018)
20. A.Ballesteros-Coll, U. Fernandez-Gamiz, I. Aramendia,E. Zulueta, and J. M. Lopez-Guede, *Energies,***13**, 3710(2020).

21. Selvarajan, L., Venkataramanan, K.b; 2 | Rajavel, R.c | Senthilkumar, T.S., Journal of intelligent and fuzzy systems, 44, 6 (2023).

22. Senthil Kumar, S., Sudhakara Pandian, R., Pitchipoo, P., Senthilkumar, T. S., Ponnambalam, S. G., Journal of testing and evaluation, 51, 2 (2022).

23. L, S., K, V. & S, S.T. Silicon 15, 1747–1769 (2023).

24. T.S. Senthilkumar1, S. Rathinavel, S. Senthil Kumar, A. Ganesh babu, Tierärztliche Praxis, 41 (2021).

25. R. Yokeswaran, V. Vijayan, T. Karthikeyan, B. Suresh Kumar, G. Sathish Kumar, Journal of New Materials for Electrochemical Systems, 22, 1 (2019).

26. R. Yokeswaran, V. Vijayan, T. Karthikeyan, M. Loganathan and A. Godwin Antony, Journal of New Materials for Electrochemical Systems, 23, 4 (2020).

27. Radha krishnan B, Vijayan V. Authorea. (2020).

28. S. Baskar, L. Karikalan, V. Vijayan, D. Arunkumar, K. Sukenraj, Materials Today: Proceedings, 37, 2 (2021).